Carbohydrate Polymers 78 (2009) 926–931

Contents lists available at ScienceDirect

Carbohydrate Polymers

journal homepage: www.elsevier.com/locate/carbpol

Development of novel α-chitin/nanobioactive glass ceramic composite scaffolds for tissue engineering applications

Mathew Peter [a], Pandian Thodi Sudheesh Kumar [a], Nelson Sathy Binulal [a], Shanti V. Nair [a], Hiroshi Tamura [b], Rangasamy Jayakumar [a,*]

[a] Amrita Centre for Nanosciences, Amrita Institute of Medical Sciences and Research Centre, Amrita Viswa Vidyapeetham University, Kochi 682026, India
[b] Faculty of Chemistry, Materials and Bioengineering & High Technology Research Centre, Kansai University, Osaka 564-8680, Japan

ARTICLE INFO

Article history:
Received 17 June 2009
Received in revised form 24 June 2009
Accepted 9 July 2009
Available online 14 July 2009

Keywords:
Chitin
Bioactive glass ceramic nanoparticles
Composite scaffolds
Tissue engineering
Biomaterials

ABSTRACT

Bioactive glass ceramic nanoparticles (nBGC) were prepared by sol–gel technique. The novel chitin/nBGC composite scaffolds were prepared using chitin gel with nBGC by lyophilization technique. The prepared nBGC and composite scaffolds were characterized using Transmission Electron Microscopy (TEM), Scanning Electron Microscopy (SEM), Fourier Transformed Infrared Spectroscopy (FT-IR) and X-ray diffraction (XRD). The composite scaffolds showed adequate porosity where the nBGC nanoparticles were homogenously distributed on the pore walls. The swelling, density, degradation and *in vitro* biomineralization capability of the composite scaffolds were also evaluated. The developed composite scaffolds showed adequate swelling and degradation properties along with its ability to become bioactive. Cytocompatability of the scaffolds was assessed using MTT assay, direct contact test and cell attachment studies. Results indicated no sign of toxicity and cells found to be attached to the pore walls offered by the scaffolds. These results suggested that the developed composite scaffold possess the prerequisites for tissue engineering scaffolds and it can be used for tissue engineering applications.

1. Introduction

Chitin is a natural biopolymer present in abundance in exoskeleton of insects, shell of crustaceans and on fungal cell wall. Chitin is composed of β-1, 4 glycan of *N*-acetyl-D-glucosamine units (Maeda, Jayakumar, Nagahama, Furuike, & Tamura, 2008; Nagahama et al., 2008). Chitin finds applications in various fields like cosmetics, water purification and separation material and as a food additive. Attempts have been made to use chitin for various applications like wound dressings and as scaffolds in tissue engineering due to their wound healing, antibacterial and anti-inflammatory properties (Jayakumar, Reis, & Mano, 2006; Jayakumar, Nwe, Tokura, & Tamura, 2007; Jayakumar, Selvamurugan, Nair, Tokura, & Tamura, 2008; Maeda et al., 2008). However, it has poor mechanical property. Therefore chitin can be used as bone substitute for bone repair and reconstruction only if its mechanical property can be improved with addition of biomaterials like hydroxyapatite (HA), bioactive glass ceramic etc.

Bioactive glass ceramics are a group of osteoconductive silicate based materials used for bone repair. Bioactive glass was developed by Hench as a biomaterial to repair bone defects (Hench, 1991) and is widely used in orthopaedic and dentistry. Bioactive glass ceramic coatings on the surface of titanium are superior to hydroxyapatite in their ability for osteointegration (Wheeler, Montfort, & McLoughlin, 2000). Moreover bioactive glass ceramic can also bond to soft and hard tissue (Verrier, Blaker, Maquet, Hench, & Boccaccinia, 2004). The bonding ability of these materials is attributed to the formation of carbonated apatite layer on the surface of the coated materials (Kokubo, 1991). Bioactive glass ceramics have been reported to influence osteoblast and bone marrow stromal cell proliferation and differentiation (Bosetti & Cannas, 2005; Foppiano, Marshall, Marshall, Saiz, & Tomsia, 2007). It has also been reported that bioactive glass could directly influence cells at the genetic level (Hench, 2009). Many groups have reported that bioactive glass ceramics influences osteoblastic cell differentiation with an increase in the level of differentiation markers like ALP, osteocalcin and osteopontin (Valerio, Pereira, Goes, & Leite, 2004; Xynos, Edgar, Buttery, Hench, & Polak, 2000).

Sol–gel method is a versatile technique to produce nano sized ceramic particles by tuning the precipitation reaction. Nanobioactive glass ceramic (nBGC) preparation has been reported using sol–gel method (Xia & Chang, 2007). Nanosurface and nanoparticles are known to influence cell behaviour and cell–material interactions. Hence, nanophase ceramics are better compared to microphase ceramics (Webster, Ergun, Doremus, Siegel, & Bizios 2000). Hence it is interesting to investigate the possibility of preparing chitin/nBGC composite scaffolds and its properties for tissue engineering applications. Hence in this paper, we describe the preparation of

* Corresponding author. Tel.: +91 484 2801234; fax: +91 484 2802020.
E-mail addresses: rjayakumar@aims.amrita.edu, jayakumar77@yahoo.com (R. Jayakumar).

0144-8617/$ - see front matter © 2009 Elsevier Ltd. All rights reserved.
doi:10.1016/j.carbpol.2009.07.016

chitin/nBGC composite scaffolds and its properties relevant to tissue engineering applications.

2. Experimental

2.1. Materials

α-Chitin was received from Kyowa Tecnos Co., Ltd. (Tiba, Japan) as powder. Tetraethyl orthosilicate (TEOS), calcium nitrate ($Ca(NO_3)_2{\cdot}4H_2O$), citric acid, ammonium dibasic phosphate, Poly (ethylene glycol), calcium chloride, methanol, minimum essential medium (MEM), 3-(4,5-dimethylthiazol-2-yl)-2,5-diphenyltetrazolium bromide MTT, Triton-X100, hydrochloric acid (HCl) and isopropanol was purchased from Sigma Aldrich Company. Glutaraldehyde and hen lysozyme was purchased from Fluka. Trypsin–EDTA and fetal bovine serum (FBS) were obtained from Gibco, Invitrogen Corporation.

2.2. Preparation of nBGC nanoparticles

For preparing nBGC nanoparticles, 7.639 g calcium nitrate and 9.84 ml of TEOS were dispersed in ethanol–water solution (60:120 ml). The pH of solution was adjusted in a range of 1–2 by adding citric acid and the reaction mixture was stirred until a transparent solution was obtained. A second solution was prepared by adding 1.078 g of ammonium dibasic phosphate and 15 g of Poly (ethylene glycol) (PEG Mw 20,000) into 1500 ml deionised water and then the pH of the solution was adjusted to 10 with ammonia water. Then, TEOS–$Ca(NO_3)_2$ solutions was dropped into ammonium dibasic phosphate solution under vigorous stirring and the reaction mixture was aged for 24 h at room temperature to obtain a white gel precipitate. Finally, $CaO–SiO_2–P_2O_5$ ternary nBGC were obtained by filtration, lyophilization (CHRiST ALPHA 2–4 LD Plus) and calcination of the precipitate.

2.3. Preparation of α-chitin/nBGC composite scaffolds

α-Chitin (5 g) was added to 1000 ml of saturated $CaCl_2{\cdot}2H_2O$/methanol solvent and blended at 15,700 rpm using a blender. The solution was agitated till a transparent chitin solution was obtained. Then the solution was filtered solution using Whatman filter paper. The filtered solution was then dialysed against distilled water to remove the calcium ions. The resultant chitin hydrogel was mixed with 1% nBGC and stirred for 24 h. After stirring for 24 h, the hydrogel was transferred into a 24 well culture plate and pre-freezed at −20 °C for 12 h. Then the freezed hydrogel was lyophilized at −80 °C for 48 h to obtain the composite scaffolds.

2.4. Characterization

The morphology and size of nBGCs assessed using TEM (JEOL JEM2100F) by dispersing in ethanol. The structural morphology of the composite scaffolds was examined using scanning electron microscope (SEM). Composite scaffold samples were prepared by taking thin sections with a razor blade. The sections were platinum sputtered in vaccum (JEOL, JFC-1600, Japan), and examined using scanning electron microscope (JEOL, JSM-6490LA, Japan).

Infra red (IR) spectra of dried nBGC and composite scaffolds were characterized using a FTIR spectrometer (Perkin–Elmer RX1). Dried nBGC and composite scaffolds were ground and mixed thoroughly with potassium bromide at a ratio of 1:5 (sample: KBr) and pelleted. The IR spectra of the pellets were then analysed at range of 400–4000 cm^{-1}. XRD patterns of composite scaffolds and nBGC were analysed at room temperature using a Panalytical diffractometer (XPERT PRO powder) (Cu Kα radiation) operating at a voltage of 40 kV. XRD were taken 2θ angle range of 5–60° and the process parameters were: scan step size 0.02 (2θ) and scan step time 0.05 s. Energy-dispersive X-ray spectroscopy (EDS) analysis was performed on JEOL JSM 6490 LA. The sample was then platinum coated with JEOL JFC 1600 for 2 min for 10 mA.

2.5. Density

To determine the density of scaffold, three scaffolds were selected and measurement was performed on an analytical balance equipped with a density determination kit (Sartorius YDK 01). Density measurements were done with ethanol as the displacement medium. Ethanol did not cause a change in pore size hence used as displacement medium.

2.6. Swelling studies

The swelling studies were performed in PBS at pH 7.4 at 37 °C. The dry weight of the scaffold was noted (Wo). Scaffolds were placed in PBS buffer solution at pH 7.4 for 1 h at 37 °C and then removed. The surface adsorbed water was removed by filter paper and wet weight was recorded (Ww). The ratio of swelling was determined using the following formula.

$$\text{Swelling Ratio} = Ww - Wo/Wo$$

2.7. In vitro degradation studies

The degradation pattern of the composite scaffold was studied in PBS medium containing lysozyme at 37 °C. Three scaffolds were immersed in lysozyme (10,000 U/ml) containing medium and incubated at 37 °C for 7 days. After 7 days, scaffolds were washed in deionised water to remove ions adsorbed on surface and were freeze dried. Initial weight of the scaffold was noted as Wo and dry weight as Wt. The degradation of scaffolds was calculated using the following formula.

$$Degradation\% = Wo - Wt/Wo \times 100$$

2.8. In vitro biomineralization studies

Three scaffolds of equal weight and shape was immersed in 1× simulated body fluid (SBF) (Kokubo & Takadama, 2006) solution and then incubated at 37 °C in closed Falcon tube for 7 days. After specified time, scaffolds were removed washed three times with deionised water to remove adsorbed minerals. Finally the scaffolds were lyophilized, sectioned and viewed using SEM for mineralization.

2.9. Cell culture studies

Cell studies were conducted using osteoblast like cells (MG-63). Cell lines were maintained in the cell culture facility in MEM with 10% FBS and 100 U/ml penicillin–streptomycin. Cells were detached from the culture plate at 80–85% confluency and used for seeding on the scaffolds for investigating the cytocompatibility of composite scaffolds. Prior to cell seeding, scaffolds were sterilized using ethanol/UV treatment and incubated with culture medium for 1 h at 37 °C in a humidified incubator with 5% CO_2 and 85% humidity. Cells were seeded drop wise onto the top of the scaffolds (1×10^5 cells/100 μl of medium/scaffold), which fully absorbed the media, allowing cells to distribute throughout the scaffolds. Subsequently, the cell-seeded scaffolds were kept at 37 °C in the CO_2 incubator under standard culturing conditions for 4 h in order to allow the cells to attach to the scaffolds. After 4 h, scaffolds were fed with additional culture medium.

2.10. Cytocompatability of the scaffolds

The viability of cells grown on the scaffolds was determined using the colorimetric MTT (3-(4,5-dimethylthiazol-2-yl)-2,5-diphenyltetrazolium bromide) assay. MTT assay measures the reduction of the tetrazolium component MTT by viable cells. Therefore, the level of reduction in MTT into formazan can reflect the level of cell metabolism. For the assay, cells were seeded on 96 well plates at a density of 10^4 cells/well and were incubated under standard culturing conditions. Extract from the scaffolds were prepared by incubating the pre-sterilized scaffolds incubated in culture medium as per ISO specification 10993-5 (i.e. 60 cm^2 per 20 ml of medium for 48 h at 37 °C with agitation) and the medium with leachables was collected in a falcon tube. Culture media of the seeded cells were replaced after 24 h by the extract (media with the leachables). Cells were incubated on the extract for 48 h. After the incubation period, the extract was replaced by fresh media containing 10% of MTT solution. After that, plate was incubated at 37 °C in humidified atmosphere for 4 h. Then the medium was removed, 100 μl of solubilization buffer (Triton-X100, 0.1 N HCl and isopropanol) was added to each well to dissolve the formazan crystals. The absorbance of the lysate was measured in a microplate reader (biotek) at a wavelength of 570 nm.

Direct contact test was performed to show cytocompatability of the scaffolds placed in direct contact with cells. Cells were grown as monolayer on culture dishes and pre-sterilized scaffolds were placed and incubated for 24 h in direct contact to monolayer of cells. After the incubation period, scaffolds were removed from the monolayer of cells and images of the monolayer of cells were acquired with an inverted microscope (Leica) attached with a CCD camera.

2.11. Cell morphology on the scaffolds

Morphology and spreading pattern of cells on the composite scaffolds were evaluated 12 h after seeding, using SEM. For SEM analysis, cell seeded composite scaffolds were fixed with 2.5% glutaraldehyde, rinsed with PBS and dehydrated using graded series of ethanol (25–100%). The samples were coated with platinum and examined under SEM.

3. Results and discussion

3.1. Characterization

Fig. 1a shows the TEM image of prepared nBGC nanoparticles. The particles had rod shaped morphology and the particle size was around 100 nm. They showed uniformity in shape and size. Fig. 1b shows the EDS spectra of the prepared nBGC nanoparticle. EDS spectrum shows the peaks of Ca, P, Si, and O. The atomic ratio of Si:Ca:P:O was found to be 43:34:6:17 as determined by EDS. These results confirmed the nanoscale size and composition of nBGC.

The FT-IR studies of nBGC and composite scaffolds are shown in Fig. 2(A). The FT-IR spectrum of chitin shows a peak at 1654 cm^{-1}, which corresponds to the primary amide groups of chitin (Fig. 2(A) a) (Jang, Kong, Jeong, Lee, & Nah, 2004). FT-IR spectra of nBGC showed vibration bands at 467 and a shoulder at 1200 cm^{-1} are assigned to Si–O–Si bending mode (Fig. 2(A) b). A vibration band at 1070 cm^{-1} and a double peak at 607 and 567 cm^{-1}, which were present, are associated with the stretching vibration of phosphate groups (Xia & Chang, 2007). The new vibration bands at 467 cm^{-1} was also observed in the composite scaffolds which was due to Si–O–Si bending mode of nBGC present in the composite scaffolds (Fig. 2(A) c).

The XRD spectra of nBGC and composite scaffold are shown in Fig. 2(B) The XRD studies confirmed that the calcinated glass generally existed in amorphous state and no diffraction peaks could be observed except a broad band between 15° and 40° (2θ) (Fig. 2(B) a) (Xia & Chang, 2007). The XRD spectrum of chitin showed two peaks at 9.1° and 21.1° (2θ) (Fig. 2(B) b) (Jang et al., 2004). XRD of composite scaffold showed a broad peak at 21.5^0, which is attributed to chitin in the scaffold (Fig. 2(C) c).

SEM micrograph of the composite scaffolds (Fig. 3) showed that scaffolds were macro porous in nature. nBGC particles were seen on the walls of the composite scaffold and were uniformly dispersed in the matrix. Pore size of CG & CG/nBGC scaffold varied from 150 to 500 μm as measured by SEM. For tissue engineering scaffolds the ideal pore size range 150–200 μm as reported earlier. This suggests that the pore size of the composite scaffolds is ideal for tissue engineering applications.

3.2. Density

The density of three composite scaffold samples is shown in Fig. 4a. The density studies were performed in ethanol, as the displacement medium as the chitin scaffolds tends to swell in water. Ethanol does not change the pore size or porosity. The densities of the samples were rather uniform suggesting that by lyophilization we can obtain scaffolds with similar porosity.

3.3. Swelling studies

Fig. 4b shows the swelling behaviour of the composite scaffolds. The results suggest that the composite scaffolds showing

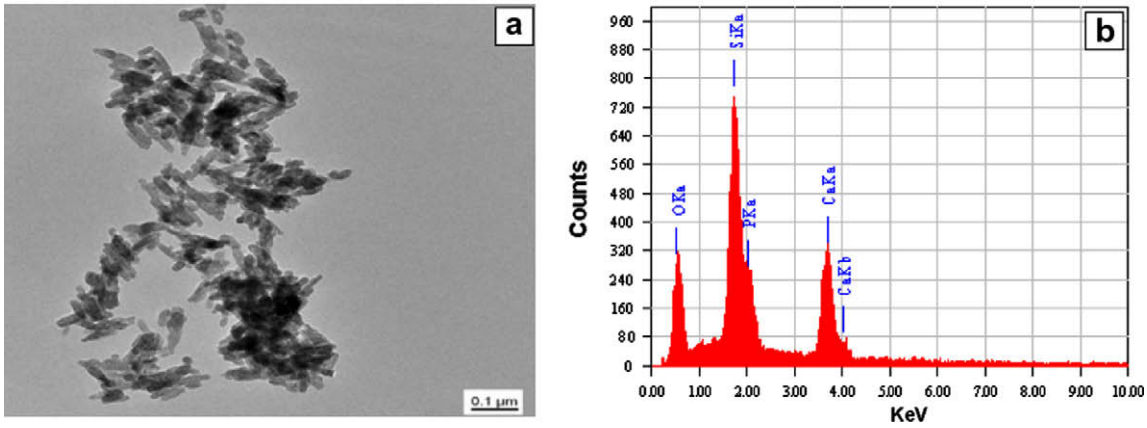

Fig. 1. (a) TEM micrograph showing the spherical shape of the nanoparticles with an average particle size below 100 nm. (b) EDS spectra of nBGC showing the peaks of Si, Ca, P and O.

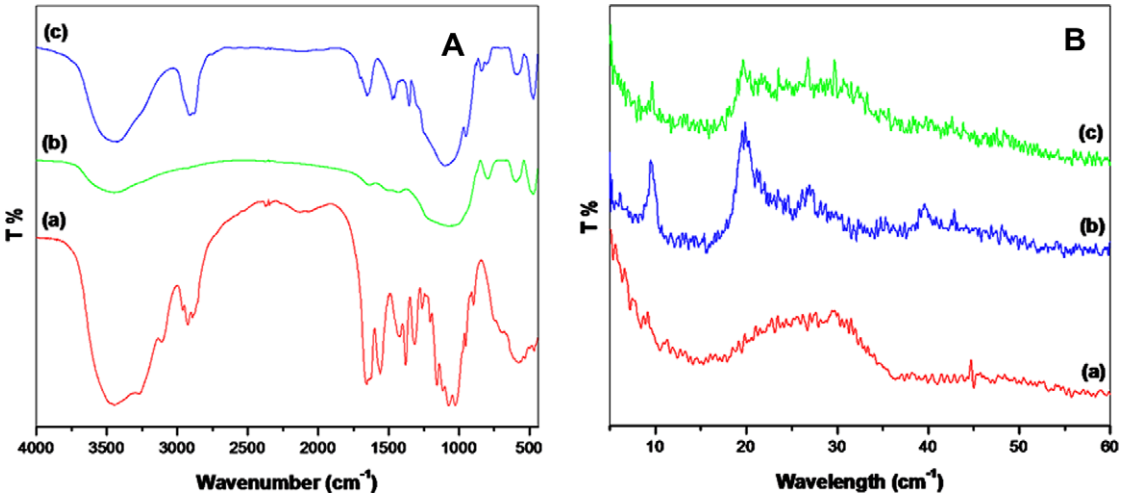

Fig. 2. (A) FT-IR spectra of (a) Chitin (b) nBGC (c) Chitin/nBGC scaffolds. (B) XRD patterns of (a) nBGC, (b) Chitin and (c) Chitin/nBGC scaffolds.

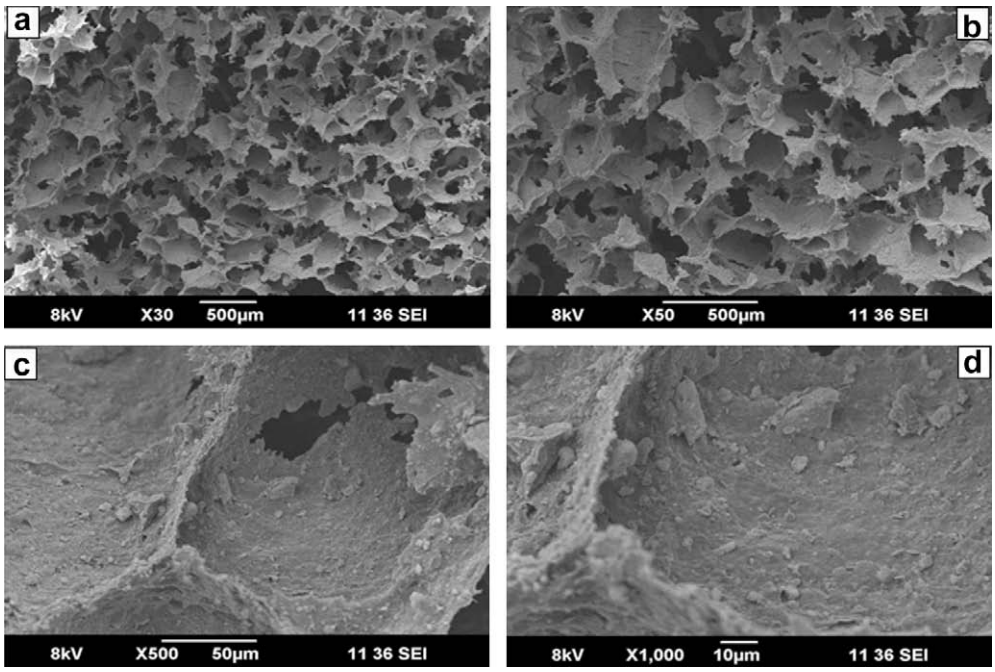

Fig. 3. (a–d) SEM images of the macro porous structure of the composite scaffolds. Pore size ranged from 150 to 500 µm.

controlled swelling behaviour in PBS medium. Swelling causes an increase in the pore size and porosity, which aids in the supply of nutrients and oxygen to the interior regions of the composite scaffolds. It also increases the surface area allowing for cells to adhere to the surface of the composite scaffolds.

3.4. In vitro degradation studies

The *in vitro* degradation profile of three composite scaffolds is shown in Fig. 4c. Chitin can be degraded by lysozyme enzyme present in human body. The results showed that the composite scaffolds losses 6–7% of their weight after 1 week incubation with lysozyme. The degradation studies shows that the composite scaffolds are biodegradable. Hence, these composite scaffolds can be used for tissue engineering application. An ideal scaffold should be biodegradable and rate of degradation should match the tissue regeneration.

3.5. In vitro biomineralization studies

The *in vitro* biomineralization of scaffolds immersed in 1X SBF after 7 days is shown in Fig. 5a. The SEM images showed the deposition of apatite on the surface of the composite scaffolds. The XRD studies of the mineralized scaffolds showed a sharp peak at 31.7° (2θ) attributed to 211 plane of hydroxyapatite (Jayakumar et al., 2009; Madhumathi et al., 2009a, 2009b) (Fig. 5b). Both these results showed the bioactive nature of the composite scaffolds. The biominearlization studies suggested that scaffolds might be ideal for cells to deposit extra cellular matrix of bone composed of inorganic apatite.

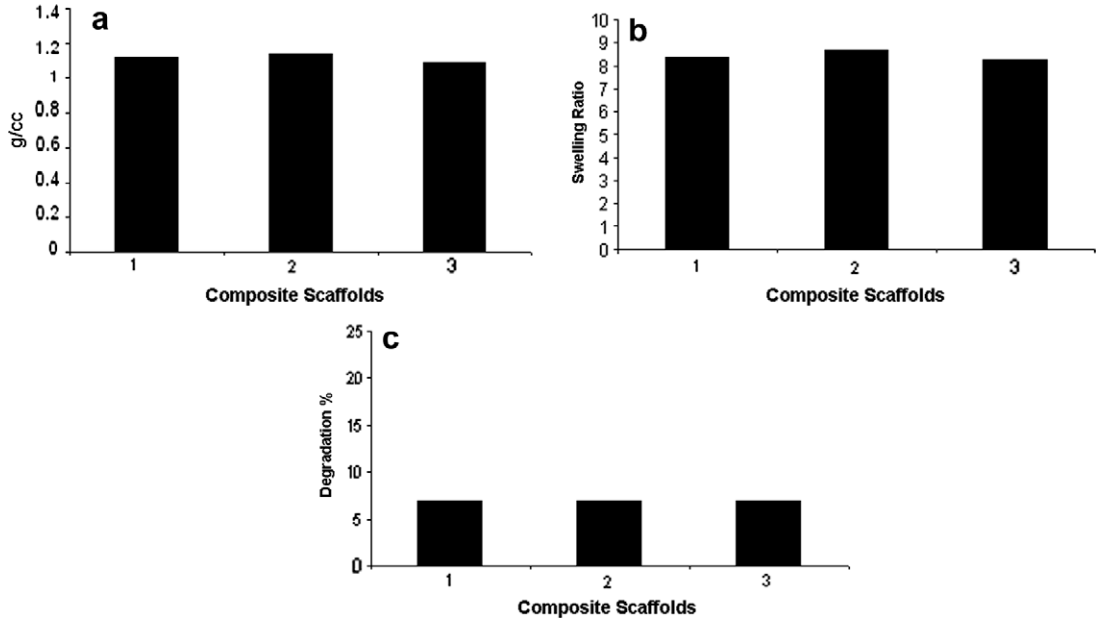

Fig. 4. (a) The density study of the composite scaffolds, (b) swelling behaviour of the composite scaffolds and (c) The *in vitro* degradation studies of composite scaffolds in lysozyme solution.

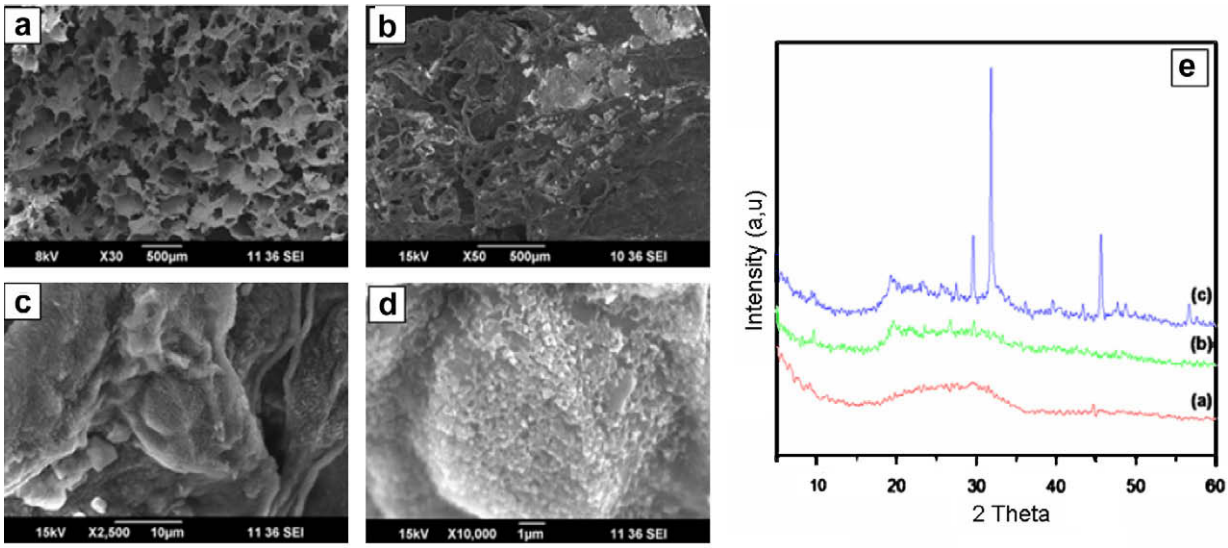

Fig. 5. *In vitro* biomineralization studies on the composite scaffolds after 7 days (a) control, (b–d) mineralised scaffolds. (5e) XRD spectrum of (a) nBGC (b) control and (c) after immersing 7 days in SBF.

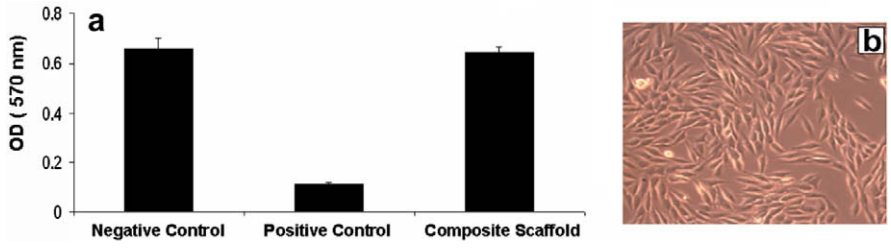

Fig. 6. (a) MTT assay showing biocompatibility of the composite scaffolds (b) the morphology of cells grown in direct with cells.

3.6. Cytocompatibility of composite scaffolds

The cytocompatability of the composite scaffolds was assessed using MTT assay and direct contact test. The assay results showed that there was no significant decrease in the OD values in cells treated with extract (Fig. 6a). This suggests that the developed composite scaffolds have no cytotoxic leachables therefore it is cytocompatible. The direct contact test results showed that, cells

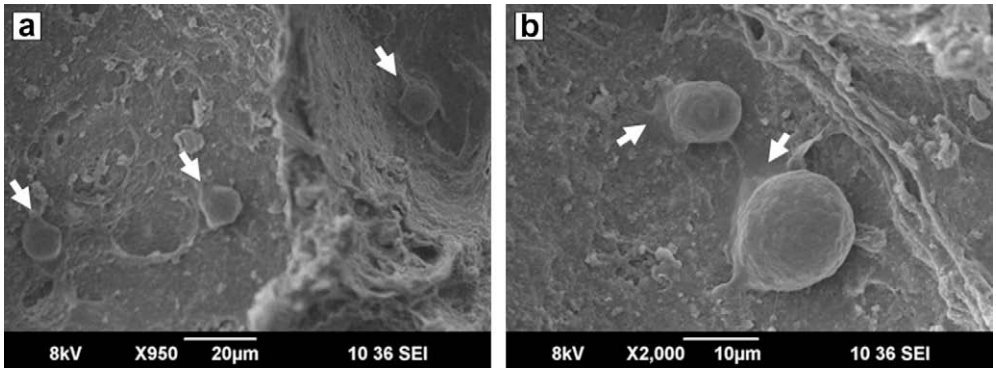

Fig. 7. (a) The SEM image of cells attached to pore walls of composite scaffolds (white arrows) and (b) higher magnification images showing initial signs of cell spreading (white arrows).

retained the characteristic morphology of MG-63 cell line when cultured in direct contact with cells (Fig. 6b). These results suggests that the composite scaffolds are cytocompatible and can be used for tissue engineering applications.

3.7. Cell attachment studies

SEM was used to characterize the morphology of cells seeded on the composite scaffolds. Cells were found attached to the pore walls offered by the composite scaffolds (Fig. 7a). They showed globular morphology with the initial signs of spreading after 12 h of incubation as shown in Fig. 7 (b). These results suggests that the composite scaffolds provided a suitable environment for cell adhesion. The present study was focused on the development and characterization of composite scaffolds for tissue engineering applications. Cell proliferation and differentiation studies are under way to fully understand the potential of these composite scaffolds for tissue engineering applications. The preliminary results suggested that the composite scaffolds could be used for tissue engineering applications.

4. Conclusions

Novel chitin/nBGC composite scaffolds were prepared using chitin hydrogel with nBGC. The composite scaffolds were macroporous in nature and pore size ranged from 150 to 500 μm. The swelling studies showed that the scaffolds absorb water and swell, which may promote cell adhesion. The scaffolds were biodegradable and lost 6–7% of their initial weight after 7 days incubation with lysozyme. Biomineralization studies showed the deposition of apatite on the surface of the scaffolds suggesting the bioactive nature of the scaffolds. The biocompatibility results showed that composite scaffolds were biocompatible. Cells seeded on the composite scaffolds attached to the pore walls of the scaffolds and showed initial signs of spreading at 12 h. Therefore we concluded that chitin/nBGC composite scaffolds could be used for tissue engineering applications.

Acknowledgements

The Department of Science and Technology, Government of India supported this work, under a centre grant of the Nanoscience and Nanotechnology Initiative program monitored by Dr. C.N.R. Rao. The authors are thankful to Prof. Greta R. Patzke, Institute of Inorganic Chemistry, University of Zurich for helping in TEM studies. The authors are also thankful to Mr. Sajin. P. Ravi for his help in SEM studies.

References

Bosetti, M., & Cannas, M. (2005). The effect of bioactive glasses on bone marrow stromal cells differentiation. *Biomaterials, 26*, 3873–3879.
Foppiano, S., Marshall, S. J., Marshall, G. W., Saiz, E., & Tomsia, A. P. (2007). Bioactive glass coatings affect the behaviour of osteoblast-like cells. *Acta Biomaterialia, 3*, 765–771.
Hench, L. L. (1991). Bioceramics: From concept to clinic. *Journal of American Ceramic Society, 74*, 1487–1510.
Hench, L. L. (2009). Genetic design of bioactive glass. *Journal of the European Ceramic Society, 29*, 1257–1265.
Jang, M. K., Kong, B. G., Jeong, Y. I., Lee, C. H., & Nah, J. W. (2004). Physiochemical characterization of α-chitin, β-chitin, γ-chitin separated from natural resources. *Journal of Polymer sciences: Part A, 42*, 3423–3432.
Jayakumar, R., Reis, R. L., & Mano, J. F. (2006). Chemistry and applications of phosphorylated chitin and chitosan. *E-Polymers*, 035.
Jayakumar, R., Nwe, N., Tokura, S., & Tamura, H. (2007). Sulfated chitin and chitosan as novel biomaterials. *International Journal of Biological Macromolecules, 40*, 175–181.
Jayakumar, R., Selvamurugan, N., Nair, S. V., Tokura, S., & Tamura, H. (2008). Preparative methods of phosphorylated chitin and chitosan – An overview. *International Journal of Biological Macromolecules, 43*, 221–225.
Jayakumar, R., Rajkumar, M., Freitas, H., Sudheesh Kumar, P. T., Nair, S. V., Furuike, T., et al. (2009). Bioactive and metal uptake studies of carboxymethyl chitosan-graft-D-glucuronic acid membranes for tissue engineering and environmental applications. *International Journal of Biological Macromolecules, 45*, 135–139.
Kokubo, T. (1991). Bioactive glass ceramics: Properties and applications. *Biomaterials, 12*, 155–163.
Kokubo, T., & Takadama, H. (2006). How useful is SBF in predicting in-vivo bone activity? *Biomaterials, 27*, 2907–2915.
Maeda, Y., Jayakumar, R., Nagahama, H., Furuike, T., & Tamura, H. (2008). Synthesis, characterization and bioactivity studies of novel β-chitin scaffolds for tissue-engineering applications. *International Journal of Biological Macromolecules, 42*, 463–467.
Madhumathi, K., Binulal, N. S., Nagahama, H., Tamura, H., Shalumon, K. T., Selvamurugan, N., et al. (2009a). Preparation and charaterization of novel-chitin-hydroxyapatite composite membranes for tissue engineering applications. *International Journal of Biological Macromolecules, 44*, 1–5.
Madhumathi, K., Shalumon, K. T., Divya Rani, V. V., Tamura, H., Furuike, T., Selvamurugan, N., et al. (2009b). Wet chemical synthesis of chitosan hydrogel-hydroxyapatite composite membranes for tissue engineering applications. *International Journal of Biological Macromolecules, 45*, 12–15.
Nagahama, H., Kashiki, T., Nwe, N., Jayakumar, R., Furuike, T., & Tamura, H. (2008). Preparation of biodegradable chitin/gelatin membranes with GlcNAc for tissue engineering applications. *Carbohydrate Polymers, 73*, 456–463.
Verrier, S., Blaker, J. J., Maquet, M., Hench, L. L., & Boccaccinia, R. A. (2004). PDLLA/Bioglasss composites for soft-tissue and hard-tissue engineering: An in vitro cell biology assessment. *Biomaterials, 25*, 3013–3021.
Valerio, P., Pereira, M. M., Goes, A. M., & Leite, F. (2004). The effect of ionic products from bioactive glass dissolution on osteoblast proliferation and collagen production. *Biomaterials, 25*, 2941–2948.
Wheeler, D. L., Montfort, M. J., & McLoughlin, S. W. (2000). Differential healing response of bone adjacent to porous implant coated with hydroxyapatite and bioactive glass. *Journal of Biomedical Materials Research, 55*, 603–612.
Webster, T. J., Ergun, C., Doremus, R. H., Siegel, R. W., & Bizios, R. (2000). Enhanced functions of osteoblasts on nanophase ceramics. *Biomaterials, 21*, 1803–1810.
Xynos, I. D., Edgar, A. J., Buttery, L. D. K., Hench, L. L., & Polak, J. M. (2000). Ionic products of bioactive glass dissolution increase proliferation of human osteoblasts and induce insulin-like growth factor II mRNA expression and protein synthesis. *Biochemical and Biophysical Research Communication, 276*, 461–465.
Xia, W., & Chang, J. (2007). Preparation and characterization of nano-bioactive-glasses (NBG) by a quick alkali-mediated sol–gel method. *Materials Letters, 61*, 3251–3253.